Bull Soc Chim Fr (1997) 134, 593-599

Interaction of solvent with the ground and excited state of 2- and 4-[4-(dimethylamino)styryl]-1-alkylpyridinium iodides: an absorption and fluorescence study

Ibrahim AZ Al-Ansari

Department of Chemistry, Faculty of Science, University of Qatar, PO Box 2713, Doha-Qatar

(Received 3 March 1997; accepted 12 June 1997)

Summary — The absorption and emission characteristics of four organic salts: 4-[4-(dimethylamino)styryl]-1-alkylpyridinium iodides **1–3** (alkyl: **1** = methyl, **2** = ethyl, **3** = isopropyl) and 2-[4-(dimethylamino)styryl]-1-methylpyridinium iodide **4**, in various solvents have been studied. It was found that these salts emit a single emission band which is dependent on the solvent's hydrogen bonding and polarity. In polar solvents a marked hypsochromic shift in absorption was observed, while no solvatochromism was observed in the emission spectra. A mechanism is proposed to explain these observations. In the salts **1–3** alkyl substitution on the pyridinium ring does not produce significant changes in their spectral properties. Acceptable correlations were obtained for the singlet excitation energies with the redox-potential differences of dyes **1–4**.

absorption / emission / hydrogen-bonding / solvatochromism / redox-potential

Résumé — **Interaction solvant–état fondamental–état excité des 2- et 4-[4-(diméthylamino)styryl]-1-alkylpyridinium iodures : étude de l'absorption et de la fluorescence.** Les caractéristiques de l'absorption et de l'émission de quatre sels organiques, 4-[4-(diméthylamino)styryl]-1-alkylpyridinium iodures **1–3** (alkyl : **1** = méthyl, **2** = éthyl, **3** = isopropyl) et 2-[4-(diméthylamino)styryl]-1-méthylpyridinium iodure **4**, ont été étudiés dans différents solvants. Il a été montré que ces sels émettent une bande d'émission indépendante des liaisons hydrogène du solvant et de sa polarité. Dans des solvants polaires, un déplacement hypsochrome marqué a été observé dans le spectre d'émission. Un mécanisme a été proposé pour expliquer ces observations. Dans les sels **1–3**, la substitution par le reste alkyl sur le cycle pyridinium ne produit aucun changement significatif dans leurs propriétés spectrales. Des corrélations ont été obtenues entre les énergies d'excitation de l'état singulet avec les différences de potentiel rédox des composés **1–4**.

absorption / émission / liaison hydrogène / potentiel rédox

Introduction

Compounds which consist of donor and acceptor groups, separated by a conjugated bridge, have been the subject of intensive research in order to gain information on how the variations of donor or/and acceptor moieties influence their physical and spectroscopic properties [1–3].

These compounds are of interest for their wide applications as nonlinear optical material [4, 5], dye material [6] and fluorescent polarity probe [7]. Compounds such as cyanine, merocyanine and styryl dyes, attracted attention mostly for their significant applications as sensitisers in photographic industry as well as photovoltaic devices [8]. Such dyes are shown to have voltage-dependent changes in their transmittance or fluorescence [9]. Studies also focus on their thermal isomerization [10–13] and electrical properties [14].

Here, we present a detailed analysis of the solvatochromism in both the ground and excited state, along with an examination of the redox properties of 4-[4-(dimethylamino)styryl]-1-alkylpyridinium iodides **1–3** (alkyl: **1** = methyl, **2** = ethyl, **3** = isopropyl) and 2-[4-(dimethylamino)styryl]-1-methylpyridinium iodide **4** (structures are shown in figure 1). The effect of solvent interaction with these molecules and the influence of the alkyl substituents on their spectral properties will be examined.

Experimental section

Materials

- *General procedure for preparation of compounds 1–4*

Organic salts **1–4** are prepared following the given procedure for synthesis of merocyanine dyes [15], where *N*-alkyl γ-picolinium iodides are reacted with 4-(dimethylamino) benzaldehyde and piperidine under reflux in ethanol for 24 h. The products were collected in each case and purified by recrystallisation two times from a minimum of $MeOH/H_2O$ (1:1). The yields were 80–90%.

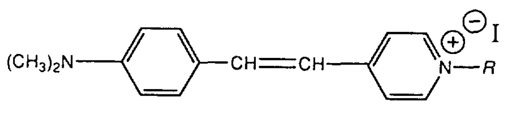

1 R = methyl
2 R = ethyl
3 R = isopropyl

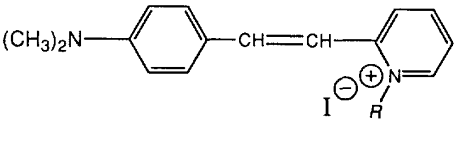

4 R = methyl

Fig 1. Structures of compounds **1–4**.

4-[4-(Dimethylamino)styryl]-1-methylpyridinium iodide ***1***

Dark metallic-maroon crystalline solid, Mp 251–255 °C.

^{1}H NMR (DMSO-d_6) δ 3.022 (s, 6H), 3.326 (s, 6H), 4.186 (s, 3H), 6.739–6.827 (d, 2H) 7.091–7.256 (d, 2H, J = 16.0 Hz), 7.561–7.649 (d, 2H), 8.021–7.845 (d, 2H), 8.661–8.728 (d, 2H).

Anal calc for $C_{16}N_2H_{19}I$: C, 52.47; N, 7.65; H, 5.23. Found: C, 52.34; N, 7.52; H, 5.50.

4-[4-(Dimethylamino)styryl]-1-ethylpyridinium iodide ***2***

Metallic-red crystalline, Mp 255–256 °C.

^{1}H NMR (DMSO-d_6) δ 1.439, 1.513 and 1.585 (t, 2H), 3.027 (s, 6H), 3.487 (s, 6H), 4.363-4.579 (q, 1H), 6.746-6.835 (d, 2H), 7.1087-7.269 (d, 2H, J = 16.13 Hz), 7.577-7.659 (d, 2H), 8.049-8.1187 (d, 2H), 8.774-8.843 (d, 2H).

Anal calc for $C_{18}N_2H_{23}I$: C, 54.83; N, 7.10; H, 5.88. Found: C, 54.80; N, 7.13; H, 5.88.

4-[4-(Dimethylamino)styryl]-1-isopropylpyridinium iodide ***3***

Dark metallic-maroon crystalline solid, Mp 291–293 °C.

^{1}H NMR (DMSO-d_6) δ 1.551–1.618 (d, 1H), 3.028 (s, 6H), 3.333 (s, 6H), 4.730–4.997 (h, 6H), 6.748–6.836 (d, 2H), 7.129–7.290 (d, 2H, J = 16.1 Hz), 7.580–7.668 (d, 2H), 8.056–8.125 (d, 2H), 8.857–8.926 (d, 2H).

Anal calc for $C_{17}N_2H_{21}I$: C, 53.7; N, 7.37; H, 5.57. Found: C, 53.75; N, 7.29; H, 5.77.

2-[4-(Dimethylamino)styryl]-1-methylpyridinium iodide ***4***

Red powder, Mp 270–271 °C.

^{1}H NMR (DMSO-d_6) δ 3.041 (s, 6H), 3.315 (s, 6H), 4.297 (s, 3H), 6.749–6.838 (d, 2H), 7.150–7.308 (d, 2H, J = 16 Hz), 7.676–7.714 (t, 2H), 7.763–7.849 (d, 1H), 8.721–8.786 (d, 1H).

Anal calc for $C_{16}N_2H_{19}I$: C, 52.47; N, 7.65; H, 5.23. Found: C, 52.20; N, 7.48; H, 5.39.

Solvents

Spectroscopy-grade cyclohexane (CH), chloroform, diethyl ether (anhydrous), dichloromethane, dimethylformamide (DMF), ethanol, methanol, and acetonitrile were purchased from BDH Chemical Co and used as received. Twice-distilled water was employed for the preparation of aqueous solutions.

Sample preparation

Stock solutions (10^{-4} mol) of the dyes were prepared by dissolving the accurate amount of these compounds in dichloromethane from which 1 mL was withdrawn and added to a 10 mL flask. This was then evaporated by nitrogen bubbling to leave a thin film. The desired solvent was added and completed to the mark to give 10^{-5} mole solution.

Measurements

Spectra were recorded with the following spectrometers: Bruker (90 MHz, ^{1}H), Perkin-Elmer 240B automatic analyser (elemental analysis), Shimatzu UV-160 spectrometer (UV-vis), Shimatzu RF-500 spectrometer (fluorescence and excitation spectra). Chemical shifts (δ) are in parts per million relative to Me_4Si. Emission spectra were obtained using a small-angle (22.5°) front surface excitation geometry. Excitation and emission slits were both 0.5 mm. Excitation wavelength λ_{exc} = 450 nm. Spectra were taken at 22 °C, using 1 cm matched quartz cells. Fresh solutions were used for all measurements. Fluorescence spectra were corrected for nonlinear instrument response. The experiments were carried out at room temperature (23 °C).

Slow-scan cyclic voltammetry (CV) was performed by using an Oxford Electrode Potentiostat/wave generator. Current–voltage curves were recorded on a Philips model PM 8043 recorder. Solutions for voltammetric examination contained 0.1 M of the supporting electrolyte tetrabutylammonium perchlorate ($TBABF_4$) and ca 5×10^{-4} M dye in acetonitrile solution, and were deaerated with bubbling by nitrogen prior to examination. A two-compartment, two-electrode voltammetry cell was utilised. Working electrodes were platinum disks of 1.6 mm and 10 μm diameter. All potentials were measured vs the Ag electrode as reference at 22 °C. The half-wave potential of ferrocene is 0.42 ± 0.002 V under these conditions.

Results and discussion

Absorption spectra

The absorption spectral features of compounds **1–4** in protic and aprotic polar solvents consist of three discrete bands. A relatively narrow $\pi-\pi^*$ short-wavelength absorption band centred around 210 nm, and a lower intensity $\pi-\pi^*$ transition (corresponding to the $^1L_b \leftarrow S_0$ state) consists of a series of low intensity bands in the range 220–350 nm. The third band is broad with high intensity in the range 360–600 nm (corresponding to $^1L_a \leftarrow S_0$ state), which is assigned to intramolecular charge transfer (ICT) involving the whole molecule due to participation of the electron lone pair of the amino group and terminating on the cationic pyridinium nitrogen terminal. Table I contrasts the absorption maxima of the third band in various solvents, while figure 2 shows absorption spectra in ethanol.

Table I. The longest-wavelength absorption maxima (λ_a), fluorescence maxima (λ_{fl}) and $\Delta\lambda$ (data in parentheses) of compounds **1–4** in selected solvents.

Solvent	α^a	ε^b	λ_a *(nm)*, $(\varepsilon_{max})^d$				λ_{fl} *(nm)* , $(\Delta\lambda)^e$			
			1	***2***	***3***	***4***	***1***	***2***	***3***	***4***
CH_2Cl_2	0.30	9.08	514.5 (3.1)	509.5 (6.4)	506.5 (4.4)	490.5 (1.9)	585 (70.5)	588 (78.5)	588 (81.5)	573 (82.5)
Chloroform	0.44	4.81	495.5 (3.3)	494.0 (6.7)	495.5 (5.0)	476.0 (1.8)	565 (69.5)	566 (72)	570 (74.5)	545 (89)
Acetonitrile	0.19	37.50	470 (3.1)	470.5 (6.2)	471.5 (4.4)	456.0 (2.9)	590 (120)	585 (114.5)	590 (118.5)	575 (119)
Ethanol	0.83	24.30	480 (3.2)	482.5 (6.3)	482 (4.6)	465.5 (2.7)	583 (103)	585 (102.5)	585 (103)	568 (102.5)
Methanol	0.93	32.63	479 (3.4)	481 (6.2)	481 (4.7)	464.5 (2.6)	580 (101)	580 (99)	580 (99)	565 (101)
Water	1.17	78.54	446.5 (1.0)	446.5 (2.5)	448 (1.7)	434.5 (1.2)	585 (139)	585 (138.5)	584 (136)	562 (127.5)
Methanol/HCl^c			330 (2.2)	339 (4.2)	327 (2.8)	325.5 (1.5)				

[a] Acidity of the solvent. [b] Dielectric constant of the solvent. [c] pH of the acidified methanol solution = 1.0. [d] Extinction coefficients are given in 10^{-4} M^{-1} cm^{-1}. [e] $\Delta\lambda$ (nm) = $\lambda_{fl} - \lambda_a$.

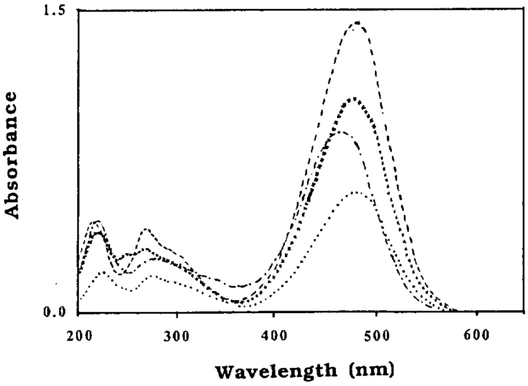

Fig 2. Absorption spectra of compounds: **1** (·····), **2** (××××), **3** (- - - -) and **4** (–·–·–) in 100% ethanol at 298 K.

The second and third bands show hypsochromic shift with the increase in acidity of the hydroxylic series of solvents and the polar protic series of solvents. In acetonitrile a strong blue shift is observed for these salts though acetonitrile has the lowest acidity (α = 0.19).

Figure 3 shows the effect of solvent variation on the absorption spectra for the salt **2** as an example.

Our results show that the blue shifts for the longest-wavelength bands (ICT transition) from dichloromethane to water are 68 nm, 63 nm, 58.5 nm and 56 nm for compounds **1–4**, respectively.

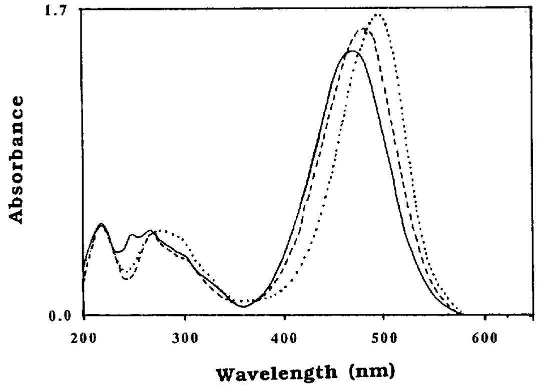

Fig 3. Absorption spectra of compound **2** in: acetonitrile (________), ethanol (- - - - -), chloroform (·········).

The charge-transfer nature of the third band is evident from the methanol acidified spectra of these compounds. It is observed that this band disappears completely on protonation of the nitrogen lone-pair, giving two broad single bands in the domain of the first two bands, but red-shifted in comparison to the spectra taken in neutral methanolic solutions (see table I).

The blue shift in the absorption spectra is consistent with the increase in the solvent acidity [16], indicating the establishment of a specific interaction via hydrogen-bonding [17–19] between the salt and the solvent. This is confirmed when the longest-wavelength absorption maxima in the polar protic and hydroxylic solvents (excluding acetonitrile) are plotted against the solvent acidities. Figure 4 shows these plots for compounds **1–4**. The abnormal behaviour of the polar acetonitrile solvent is due to the fact that it possesses both acidic

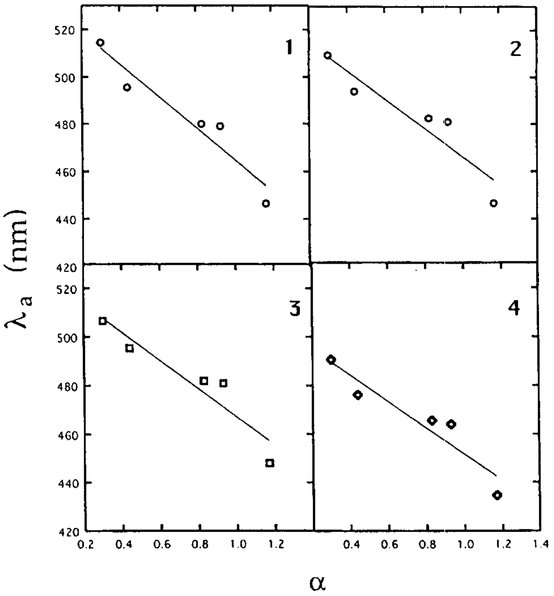

Fig 4. Plots of the longest-wavelength absorption maxima against the solvent acidity constants (α) for compounds **1–4**. The straight lines are the best fit through the data.

and basic sites (unlike dichloromethane or chloroform), thus strong hydrogen-bonds are formed between the solute molecule and a cluster of solvent molecules. This we believe to occur in hydroxylated solvents as well since they have both acidic and basic sites.

To explain this behaviour, we propose a mechanism depicted in figure 5. In this mechanism strong hydrogen bonding solvents (high acidity) stabilises structure a, thus reducing its electron-donating ability and thereby reducing the magnitude of the ICT interaction with the pyridinium moiety.

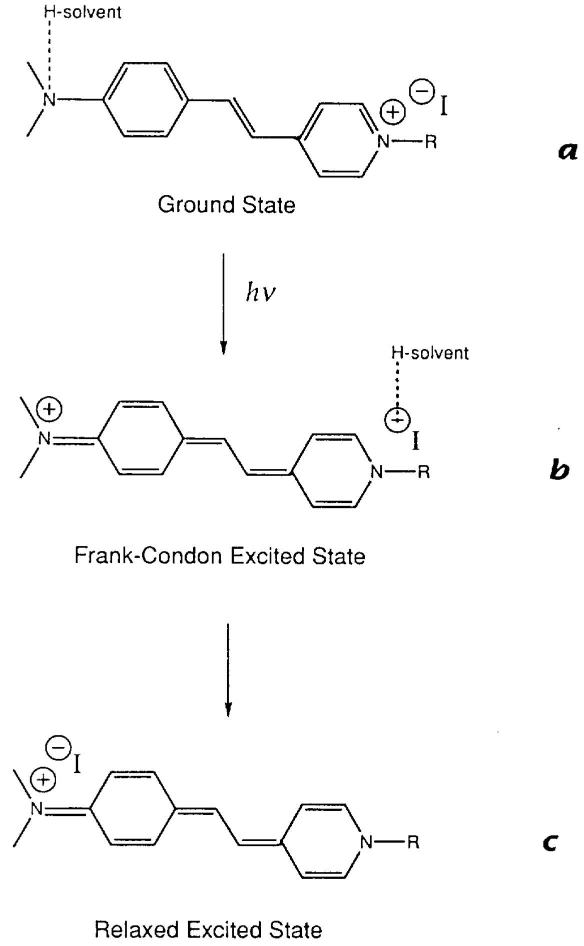

Fig 5. Schematic representation of the ground state **a**, Frank–Condon excited state **b**, and the relaxed excited state **c**.

Emission spectra

Fluorescence spectra of the salts **1–4** consist of a single broad band red-shifted from the charge transfer absorption maxima.

Examining the emission data (table I) indicates a lack of solvatochromism which suggests that the influence of the solvent polarity in stabilising the relaxed excited state is not important.

We can explain these findings based on our proposed mechanism depicted in figure 5. In the excited state, increasing the acidity of the solvent allows greater hydrogen-bonding to take place between the solvent and the iodide anion, thus stabilising structure **b**, preventing its mobility to stabilise the relaxed excited state molecule, shown as structure **c**. In this case a blue shift is expected. Our observation (table I) indicates that this is the case. The energy gap between the Frank–Condon excited state and the relaxed excited state, though being small, increases with the decrease in acidity of the solvents (compare for instance, chloroform versus dichloromethane in the moderate polar protic solvents and methanol versus ethanol). For the very high polar solvents acetonitrile and water the energy gap is very large, indicating that the polarity of these solvents plays a part in the solvation and hence dissociation of the charges in structure **b**, allowing full relaxation of the excited state.

Furthermore, comparing emissions of the relaxed excited state of compounds **1–3** in each solvent (see table I), we observe that these have the same energy. This is a manifestation that the alkyl group of the substituent does not exert any electronic inductive effect on the pyridinium moiety, an indication that our proposed mechanism for the position of charges in these salts in the fully relaxed excited state is valid.

Table II. Ground-state spectral data for **1–4** neutral radicals in acetonitrile[a].

Compound	E_s[b] *(eV)*	$E^{o'}$ *(Ox) (V)*	$E^{o'}$ *(Red) (V)*	Δ[c] *(eV)*
1	2.64	0.60	−0.90	1.14
2	2.63	0.60	−0.84	1.19
3	2.63	0.60	−0.90	1.23
4	2.72	0.70	−0.90	1.12

[a] Data obtained in CH_3CN/0.1 M $TBABF_4$; $E^{o'}$(Ox) and $E^{o'}$(Red) are reported vs Ag. [b] Singlet excitation energy corresponding to the longest-wavelength absorption maxima (λ_a). [c] Reorganization energy calculated based on the equation.

Compounds **1–3** show similarities in their emission behaviour. Within experimental error, it appears that only compound 4 is distinctly blue-shifted with respect to compounds **1–3**.

Electroreduction and electrooxidation

In order to investigate the effect of the alkyl substitution in the pyridinium acceptor group on the spectroscopic observations of compounds **1–4**, the redox potentials were examined. No CV reversible electrooxidation or electroreduction were observed. These compounds undergo an irreversible oxidation process at 0.4 V. During the cathodic portion of the voltammogram scan an oxidative sharp peak is observed for compounds **1-4** (fig 7A–D). Following the formation of the oxidised radical species, no reduction wave is observed; instead, a flat wave is seen. Our observation suggests that the oxidised products are converted to other products, mainly by dimerization [20].

A moderate broad negative formal potential for the first reduction peak appears in the anodic scan. This wave is not noticeable for compounds **1** or **2**, and to a lesser degree in the case of compounds **3** and **4**. The oxidation potentials are the same for compounds **1–3**, but lower for compound **4** (table II). However, the reduction potentials vary for compounds **1–4**, showing the following increasing order $1 = 3 = 4 < 2$.

These results indicate that alkyl substitution does not result in a significant decrease in the one-electron oxidation potentials except for compound **4**. However, an increase by 0.1 V and a shift in the CT spectral absorption maxima to shorter wavelength (by 14.5 nm) is observed for compound **4**, compared to dye **3**. On the other hand, a substantial variation in the molar absorptivity is observed in the order $4 < 1 < 3 < 2$.

These findings indicate that the rigid more localised compounds **1–3** are easily oxidised in comparison to the less conjugated compound 4. Also, it is the reduction potentials which the substituents affect mainly, due to the different degree of stability they exert on the radical-cation products formed.

Correlations between redox potentials and singlet excitation energies

The singlet excitation energy, E_S, in relation to the formal potentials is given by the following equation [21–23]:

$$E_s = [E^{\circ\prime}(\mathrm{Ox}) - E^{\circ\prime}(\mathrm{Red})] - \Delta$$

where $E^{\circ\prime}(\mathrm{Ox})$ and $E^{\circ\prime}(\mathrm{Red})$ are the formal potentials for the oxidation and reduction, respectively, and the difference $[E^{\circ\prime}(\mathrm{Ox}) - E^{\circ\prime}(\mathrm{Red})]$ is an estimate of the energy gap between the highest occupied molecular orbital (HOMO) and the lowest unoccupied molecular orbital (LUMO), and Δ is the reorganisation energy. The HOMO and LUMO energy levels relate to the gas-phase ionization potentials and electron affinities.

Interestingly, the plot of E_s vs $[E^{\circ\prime}(\mathrm{Ox}) - E^{\circ\prime}(\mathrm{Red})]$ (fig 6) exhibits a remarkable linear relationship for compounds 1–4, which shows the validity of the equation. Table II collects the singlet excitation energies, the redox potentials, reorganisation energies and the spectral data for the CT absorption bands. Our results indicate that the lowest absorption maximum is a HOMO → LUMO transition, and lowering the HOMO-LUMO gap increases the stabilization energies of the excited state, as well as the transition probabilities.

Conclusions

We have reported the absorption and fluorescence emission of four structurally similar organic salts **1–4**. We have shown that these compounds are sensitive to the acidity of the solvents. Specific interaction which was assigned to hydrogen-bonding between the solvents and these compounds leads to their spectral properties. A mechanism on the solvent's ability to form hydrogen bonding with the salt's nitrogen lone pair in the ground state and the iodide anion in the excited state is proposed. We envision that the ground state is stabilized by the solvent acidic sites. Strong hydrogen-bonding solvents prevent displacement of charge, and thus a blue shift is observed in the absorption spectra. The absence of solvatochromism in the emission is explained by this mechanism. The fully relaxed excited state is reached in solvents with low acidity, since they do not form strong hydrogen bonds with the iodide anion which is involved in stabilising this state. Strong polar solvents tend to play a role in dissociation of the charges in the excited state.

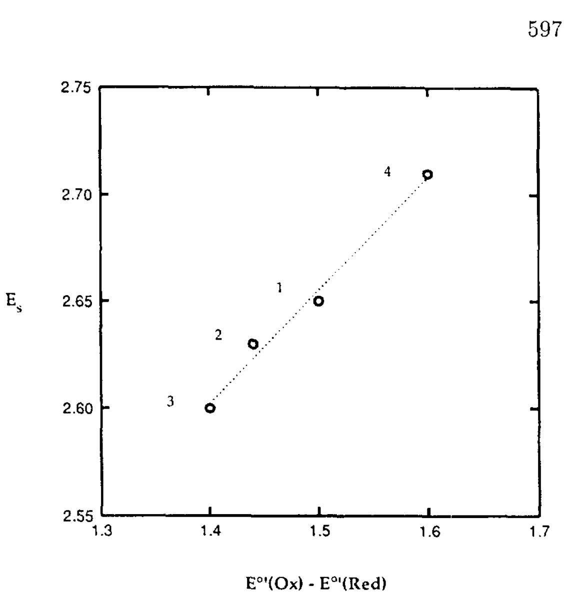

Fig 6. Plot of singlet excitation energies (E_S) of salts 1–4 vs $[E^{\circ\prime}(\mathrm{Ox}) - E^{\circ\prime}(\mathrm{Red})]$. The dotted lines are the best fit through the data.

Changing alkyl groups on the pyridinium moiety does not significantly influence the absorption or emission behaviour of these organic salts.

In this class of salts, oxidation potentials varied from 0.60 to 0.70 V. The substituents on the pyridinium cation and the molecular geometry of these salts dictate the formation of the radical-dication. These effects are manifested spectroscopically in the absorption wavelength maxima in acetonitrile and in the molar absorptivities of the charge-transfer bands.

References

1 Stiegman AE, Miskowski VM, Perry JW, Coulter DR, *J Am Chem Soc* (1987) 109, 5884

2 Slama-Schwok A, Blanchard-Desce M, Lehn JM, *J Phys Chem* (1990) 94, 3894

3 Sinha HK, Yates K, *J Am Chem Soc* (1991) 113, 6026

4 Katz HE, Singer KD, Sohn JE, Dirk CW, King LA, Gordon HM, *J Am Chem Soc* (1987) 109, 6561

5 Wilson T, Brigitte G, Joseph CC, Stevenson SH, *Chem Phys Lett* (1989) 154, 2, 93

6 Barni B, Sararino PS, Viscardi G, *Acc Chem Res* (1991) 24, 98

7 Macgregor RB, Weber G, *Nature* (1986) 319, 70

8 Chamberlin GA, Cooney PJ, Dennison S, *Nature* (1981) 45, 289

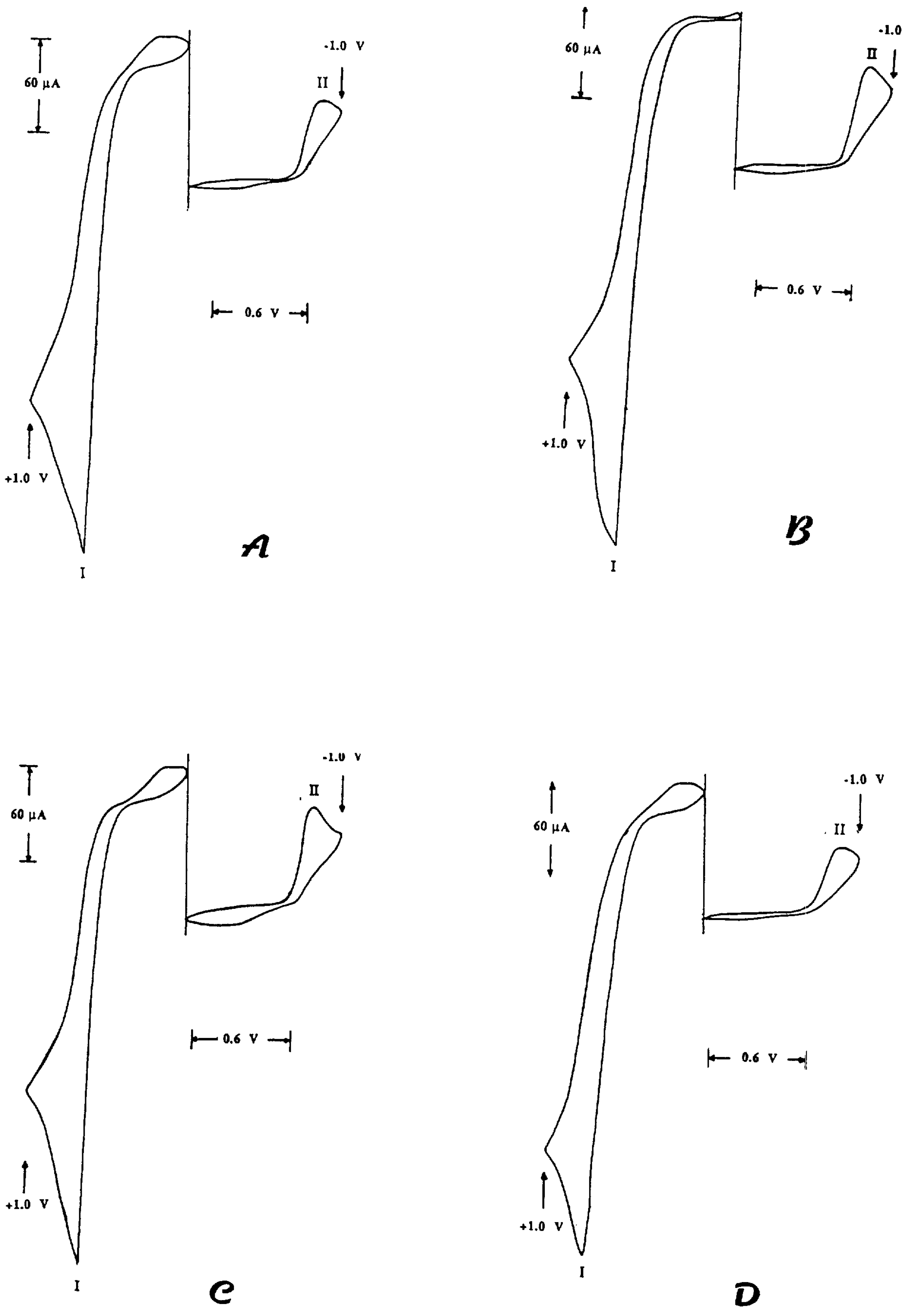

Fig 7. Cyclic voltammogram of 2 × 10^{-3} M of compounds: **1** (A), **2** (B), **3** (C) and **4** (D), recorded at Pt electrode in CH_3CN/0.35 M $TBABF_4$, scan rate = 50 mV/s. Cathodic limit = −1.0 V, anodic limit = +1.0 V.

9 Cohen LB, Salzberg BM, Davilla HV, Ross WN, Landowe D, Waggoner AS, Wang CH, *J Member Biol* (1974) 19, 1

10 Steiner U, Abel-Kader MH, Fisher P, Harmer HEA, *J Am Chem Soc* (1978) 100, 3190

11 Gorner H, *J Phys Chem* (1985) 89, 4112

12 Gorner H, Schulte-Frohlindle D, *J Phys Chem* (1985) 89, 4105

13 Gorner H, *J Phys Chem* (1987) 91, 1887

14 Etaiw SH, Ayad MM, Assar SS, *Thermochim Acta* (1990) 173, 1

15 Freeman HS, Mc Intosh SA, Clark AT, *Educ Chem* (1990) 5, 79

16 Kamlet MJ, Abboud JLM, Taft RW, *Prog Phys Org Chem* (1981) 13, 485

17 Lopez Arbeloa T, Lopez Arbeloa F, Tapia Estevens MJ, Lopez Arbeloa I, *J Phys Chem* (1993) 97, 4704

18 Lopez Arbeloa T, Lopez Arbeloa F, Tapia Estevens MJ, Lopez Arbeloa I, *J Lumin* (1994) 59, 369

19 Lopez Arbeloa T, Lopez Arbeloa F, Lopez Arbeloa I, *J Lumin* (1996) 68, 149

20 (a) Lenhard JR, Parton RL, *J Am Chem Soc* (1988) 109, 5808

(b) Parton RL, Lenhard JR, *J Org Chem* (1990) 55, 49

21 Ditchfield R, Del Bene JE, Pople JA, *J Am Chem Soc* (1972) 94, 703

22 Loutfy RO, *Can J Chem* (1976) 54, 1454

23 Chanon M, Hawley MD, Fox MA, In: *Photoinduced Electron Transfer* (Fox MA, Chanon M, Eds) (1988) Elsevier, NY, 1–59